PNAS RESEARCH ARTICLE | MEDICAL SCIENCES

Primary cilia in satellite cells are the mechanical sensors for muscle hypertrophy

Weijun Li[a,b,c], Zhenhong Zhu[a,b,d], Kai He[e], Xiaoyu Ma[e], Robert J. Pignolo[a,b], Gary C. Sieck[b], Jinghua Hu[e,1], and Haitao Wang[a,b,1]

Edited by Helen Blau, Stanford University, Stanford, CA; received February 23, 2021; accepted April 18, 2022

Skeletal muscle atrophy is commonly associated with aging, immobilization, muscle unloading, and congenital myopathies. Generation of mature muscle cells from skeletal muscle satellite cells (SCs) is pivotal in repairing muscle tissue. Exercise therapy promotes muscle hypertrophy and strength. Primary cilium is implicated as the mechanical sensor in some mammalian cells, but its role in skeletal muscle cells remains vague. To determine mechanical sensors for exercise-induced muscle hypertrophy, we established three SC-specific cilium dysfunctional mouse models—*Myogenic factor 5* (*Myf5*)-*Arf-like Protein 3* (*Arl3*)$^{-/-}$, *Paired box protein Pax-7* (*Pax7*)-*Intraflagellar transport protein 88 homolog* (*Ift88*)$^{-/-}$, and *Pax7-Arl3*$^{-/-}$—by specifically deleting a ciliary protein ARL3 in MYF5-expressing SCs, or IFT88 in PAX7-expressing SCs, or ARL3 in PAX7-expressing SCs, respectively. We show that the *Myf5-Arl3*$^{-/-}$ mice develop grossly the same as WT mice. Intriguingly, mechanical stimulation-induced muscle hypertrophy or myoblast differentiation is abrogated in *Myf5-Arl3*$^{-/-}$ and *Pax7-Arl3*$^{-/-}$ mice or primary isolated *Myf5-Arl3*$^{-/-}$ and *Pax7-Ift88*$^{-/-}$ myoblasts, likely due to defective cilia-mediated Hedgehog (Hh) signaling. Collectively, we demonstrate SC cilia serve as mechanical sensors and promote exercise-induced muscle hypertrophy via Hh signaling pathway.

primary cilia | mechanical stimulation | exercise | muscle hypertrophy

Significance

Muscle atrophy is characterized by loss of lean muscle mass and increased weakness. Physical exercise is the primary intervention to improve muscle strength and endurance in healthy individuals. However, some people are so-called exercise resistant, with underlying mechanisms unclear. We discover that the cilia of skeletal muscle satellite cells are indispensable mechanical sensors for exercise-induced muscle hypertrophy and, potentially, could be targeted for future interventions to ameliorate muscle atrophy or mimic exercise-induced beneficial effects in persons unable to exercise or responding poorly to exercise.

Exercise is considered as the primary intervention to improve muscle strength and to counteract muscle atrophy. While physical exercise training is considered a suitable intervention to improve muscle strength and endurance in healthy individuals, some people are resistant to the beneficial effects of exercise (1–3). It has been debated whether exercise is beneficial or harmful for patients with myopathic disorders (4) and type 2 diabetes (5). This so-called "exercise resistance" is considered congenital, and one recently identified causative factor involved in exercise resistance is hepatokine selenoprotein P (2, 6).

Primary cilia have a mechanosensory function in bone cells (7), renal cells (8), and airway smooth muscle cells exert a role in sensing oscillatory fluid flow and transducing extracellular mechano-chemical signals into intracellular biochemical responses (9). Intriguingly, low muscle tone is a clinical feature often present in congenital ciliopathies with unclear underlying mechanisms (10). Arf-like Protein 3 (ARL3) is a highly conserved ciliary protein across ciliated organisms. ARL3, a regulator of intraflagellar transport in primary cilia, has been reported involving with various ciliary signaling functions (11, 12) and maintaining cell division polarity (13). *Arl3* mutations cause Joubert syndrome (14, 15). *Arl3*$^{-/-}$ knockout does not affect cilia structure but compromises ciliary function (16).

Cells utilize primary cilia to convert environmental cues, mechanical or chemical, into various cellular signaling essential for development (17–21). During skeletal muscle development, Hedgehog (Hh) signaling helps to initiate the myogenic program (22). In myoblast cells, Fu et al. (23) showed that primary cilia are assembled during the initial stages of myogenic differentiation but disappear as cells progress through myogenesis. The ablation of primary cilia suppresses Hh signaling and myogenic differentiation while enhancing proliferation. However, there are still significant gaps in our understanding of how exercise and mechanical signals activate the Hh signaling pathway. In the present study, we hypothesize that primary cilia in satellite cells (SCs) transduce mechanical stimulation through activation of Hh signaling and promote muscle hypertrophy induced by exercise.

Hypertrophy of skeletal muscle is a complex biological process that involves multiple cell types, including SCs, fibro-adipogenic precursors, endothelial cells, fibroblasts, pericytes, and immune cells. Removing cilia from fibro-adipogenic precursors can reduce intramuscular adipogenesis and increase myofibril size during muscle healing (24). SCs play an essential role in muscle hypertrophy and exercise adaptation (25, 26), especially

Author affiliations: [a]Division of Geriatric Medicine & Gerontology, Department of Internal Medicine, Mayo Clinic, Rochester, MN 55905; [b]Department of Physiology and Biomedical Engineering, Mayo Clinic, Rochester, MN 55905; [c]Department of Orthopedic Surgery, The Second Affiliated Hospital, Zhejiang University School of Medicine, 310030 Hangzhou, China; [d]Orthopaedics Department, Shanghai Sixth People's Hospital, Shanghai Jiaotong University, 200240 Shanghai, China; and [e]Department of Biochemistry and Molecular Biology, Division of Nephrology and Hypertension, Mayo Clinic, Rochester, MN 55905

Author contributions: H.W. designed research; W.L., Z.Z., and K.H. performed research; X.M. contributed new reagents/analytic tools; W.L., Z.Z., K.H., R.J.P., G.C.S., J.H., and H.W. analyzed data; and W.L., R.J.P., G.C.S., J.H., and H.W. wrote the paper.

The authors declare no competing interest.

This article is a PNAS Direct Submission.

[1]To whom correspondence may be addressed. Email: Hu.jinghua@mayo.edu or Wang.Haitao@mayo.edu.

This article contains supporting information online at http://www.pnas.org/lookup/suppl/doi:10.1073/pnas.2103615119/-/DCSupplemental.

Published June 7, 2022.

in young mice (27). Mechanical signals can interrupt SC suppression in a skeletal muscle loss model induced by ovariectomy. Diminished SC number and elevated adipogenic gene expression in muscle caused by ovariectomy are averted by mechanical stimulation (28). Experiments in vitro indicate that mechanical stimulation enhances the fusion of SCs (29). SCs are a heterogeneous population of stem cells and committed progenitors (30). *Paired box protein Pax-7* (*Pax7*) is a traditional marker of SCs and acts at different levels in a nonhierarchical regulatory network controlling SC-mediated muscle hypertrophy (31). A major target gene of *Pax7* is *Myogenic factor 5* (*Myf5*), and loss of *Pax7* significantly decreases *Myf5* expression in myoblasts (32). However, *Myf5* is present in *Pax3/Pax7* double mutants, indicating *Myf5* activation occurs independently of *Pax3/Pax7* (33). Furthermore, 10% of *Pax7*-expressing satellite cells have never expressed *Myf5* (30). Parise et al. (34) observed an approximately sixfold increase in the number of Myf5-expressing cells by 48 h following exercise, which remained elevated until at least 96 h after exercise. We established three mouse models of *Myf5-Arl3*$^{-/-}$, *Pax7-Intraflagellar transport protein 88 homolog* (*Ift88*$^{-/-}$), and *Pax7-Arl3*$^{-/-}$ to investigate the SC during mechanical stimulation and exercise. In the present study, we provide exciting evidence that SC cilia act as the key mechanical sensor for exercise-induced hypertrophy.

Results

Establishment of an SC-Specific Cilium Dysfunctional Mouse Model. Our data and reports from other colleagues (23, 35) found that primary cilia are predominantly observed at the surface of human myoblasts in vitro (*SI Appendix*, Fig. S1 *A* and *E*). To check whether MYF5^{+} cells are ciliated, we isolated myoblasts from WT mouse tibialis anterior ex vivo. After confirming the isolated myoblasts are dominantly desmin-positive cells (*SI Appendix*, Fig. S2 *A* and *C*), we costained MYF5 and IFT88 or ARL13B in myoblasts in vitro (*SI Appendix*, Fig. S1 *B* and *F*), and in tissue slides from WT mouse tibialis anterior (*SI Appendix*, Fig. S1 *C* and *D*). We found that about 80% of MYF5^{+} cells are ciliated in quiescent myoblasts ex vivo. While in vivo, we found 50% of MYF5^{+} cells are ciliated cells in tissue slides (*SI Appendix*, Fig. S1 *C, D, G,* and *H*). We only counted cells with the cilia colocalized with MYF5 in the same focal plane, so the actual percentage may be higher.

Generation of the FLP-FRT conditional ARL3 knockout mouse model provided a powerful tool to investigate cilium-mediated signaling pathways (12). To study the roles of cilia in SCs during muscle growth and exercise-induced muscle hypertrophy, we bred Myf5-Cre lineage mice with *Arl3* floxed mice. We obtained a viable model: *Myf5-Arl3*$^{-/-}$ mice. The ARL3 protein was successfully abolished in *Myf5-Arl3*$^{-/-}$ myoblasts (Fig. 1*A*). We found no differences in body weight between WT and *Myf5-Arl3*$^{-/-}$ mice (Fig. 1*B*), nor significant body composition of fat and lean mass between WT and *Myf5-Arl3*$^{-/-}$ mice (Fig. 1 *C* and *D*). The percentage of ciliated myoblasts was not changed between WT and *Myf5-Arl3*$^{-/-}$ mouse models (*SI Appendix*, Fig. S2 *B* and *D*). These data indicate that *Myf5-Arl3*$^{-/-}$ mice developed normally compared to WT.

We also bred *Pax7-Cre* lineage mice with *Ift88* floxed mice. The IFT88 protein was successfully abolished in *Pax7-Ift88*$^{-/-}$ myoblasts (*SI Appendix*, Fig. S3*A*). The bodyweight of *Pax7-Ift88*$^{-/-}$ mice is decreased compared with WT mice at the age of 2 wk (*SI Appendix*, Fig. S3*B*). However, the complete anatomic dissection of *Pax7-Ift88*$^{-/-}$ mice showed hydrocephalus around the age of 2 to 3 wk (*SI Appendix*, Fig. S3*C*). Relative expression of *MyoG*, *MyoD*, and *MyHC* expression decreased in the tibialis anterior (TA) from *Pax7-Ift88*$^{-/-}$ mice compared with WT mice at the age of 2 wk using a real-time PCR test (*SI Appendix*, Fig. S3*D*).

***Myf5-Arl3*$^{-/-}$ Mice Are Not Sensitive to Exercise-Induced Muscle Hypertrophy.** When we trained 3-mo-old mice with forced exercise (treadmill testing at 10 m/min for 20 min, 5 d/wk for 4 wk), we found that the maximum speed and distance significantly increased in WT mice compared to *Myf5-Arl3*$^{-/-}$ mice (Fig. 1 *E* and *F*). *Myf5-Arl3*$^{-/-}$ mice also increased their maximum speed (but not maximum distance) after exercise training (T),

Body composition of fat and lean mass were compared before and after exercise in *Myf5-Arl3*$^{-/-}$ knockout mice and WT mice from the same litter by quantitative NMR (EchoMRI) analysis. In WT mice, the ratio of lean mass/body mass increased after 4 wk of exercise (treadmill at 10 m/min for 20 min, 5 d/wk), but this ratio was not increased in *Myf5-Arl3*$^{-/-}$ mice (Fig. 2*A*). The ratio of body fat/body mass decreased in WT mice after exercise but did not change in *Myf5-Arl3*$^{-/-}$ mice (Fig. 2*B*).

We also found that TA mass increased in WT mice but not in *Myf5-Arl3*$^{-/-}$ mice (Fig. 2*C*). After staining the muscle with Laminin (Fig. 2*D*), we quantified myofibril size using the cross-sectional area (CSA) and the minimal "Feret's diameter" of a muscle fiber cross-section. We found that exercise increased TA muscle fiber CSA in both WT and *Myf5-Arl3*$^{-/-}$ mice, but *Myf5-Arl3*$^{-/-}$ mice exhibited less exercise-induced hypertrophy compared to WT mice (Fig. 2 *E* and *F*). Intriguingly, exercise increased muscle fiber CSA in the gastrocnemius from WT, but not from *Myf5-Arl3*$^{-/-}$ mice (*SI Appendix*, Fig. S4 *A–C*). Exercise also increased muscle fiber CSA in vastus intermedius (quadriceps) from WT and *Myf5-Arl3*$^{-/-}$ mice, but WT mice exhibited more muscle hypertrophy than *Myf5-Arl3*$^{-/-}$ mice (*SI Appendix*, Fig. S4 *D–F*). These results indicate that the increased muscle fiber CSA due to the mechanical stimulation of exercise largely depends on functional cilia.

Primary Myoblast Differentiation by Mechanical Stimulation Depends on Functional Primary Cilia. We isolated primary myoblasts from WT and *Myf5-Arl3*$^{-/-}$ mice and evaluated cell differentiation in response to mechanical stimulation as a surrogate for exercise. We found that mechanical stimulation promoted myoblast differentiation into myotubes in WT mice only. The differentiation index was increased on day 1 and day 3 during myoblast differentiation. The percentage of multinucleated myosin heavy-chain (MyHC)$^{+}$ myotubes (10 or more nuclei at day 3, 20 or more nuclei at day 5) increased for WT myoblasts but not for *Myf5-Arl3*$^{-/-}$ myoblasts after mechanical stimulation (Fig. 3).

We cannot test the *Pax7-Ift88*$^{-/-}$ mice on treadmill exercise tests due to their inability to stand. However, we can still isolate their primary myoblasts to test the effect of mechanical stimulation in vitro. We found that mechanical stimulation promotes myoblast differentiation into myotubes in myoblasts derived from WT mice only. The effects of mechanical stimulation were abrogated if the *Ift88* gene was knocked out (*SI Appendix*, Fig. S5*A*). The differentiation index was increased at day 1 and day 3 during myoblast differentiation in the WT versus *Pax7-Ift88*$^{-/-}$ background. The percentage of multinucleated MyHC^{+} myotubes (10 or more nuclei at day 3, 20 or more nuclei at day 5) increased in WT myoblasts but not in *Pax7-Ift88*$^{-/-}$ myoblasts after mechanical stimulation

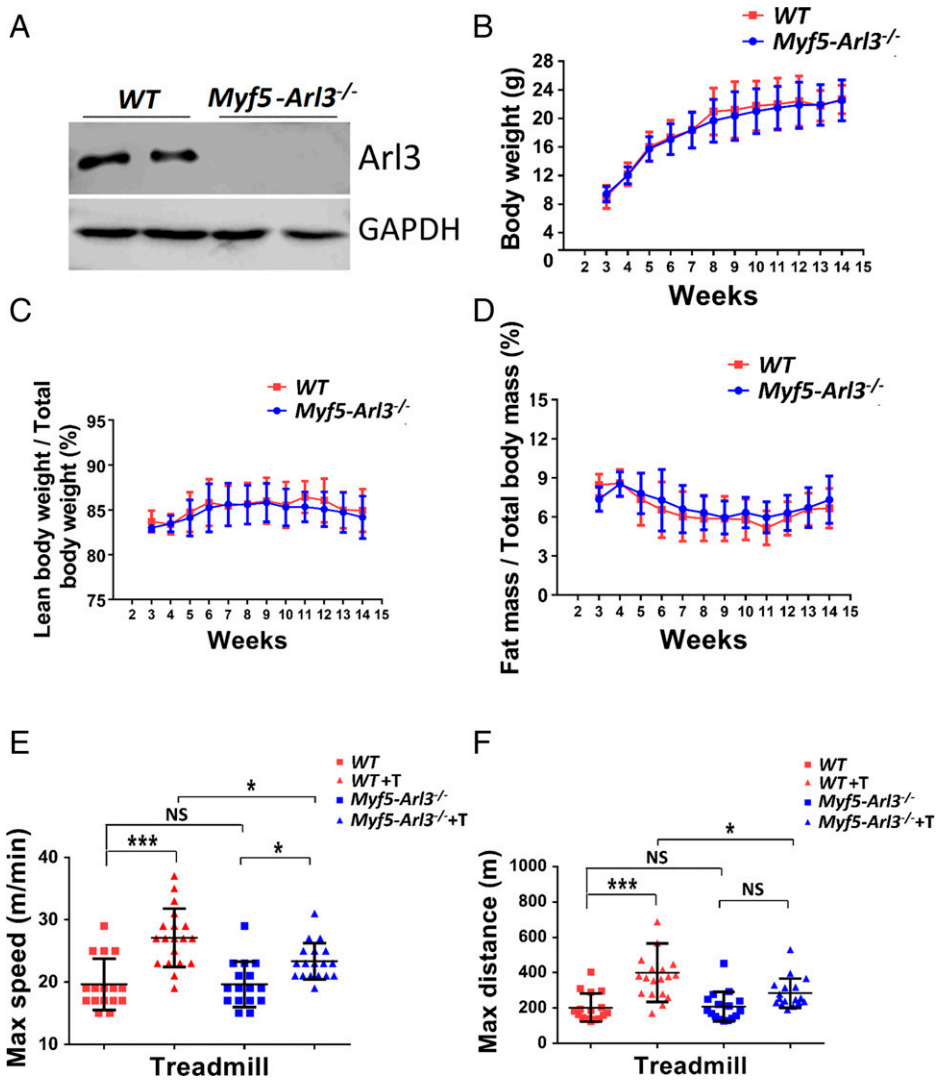

Fig. 1. Establishment of the *Myf5-Arl3*$^{-/-}$ mouse model. (*A*) The ARL3 protein was successfully abolished in *Myf5-Arl3*$^{-/-}$ myoblasts. (*B*) The bodyweight of *Myf5-Arl3*$^{-/-}$ mice is normal compared with WT mice. (*C*) The percentage of lean body weight/total body weight of *Myf5-Arl3*$^{-/-}$ mice is normal compared with WT mice. (*D*) The percentage of fat mass/total body mass of *Myf5-Arl3*$^{-/-}$ mice is normal compared with WT mice. (*E*) The maximum speed was increased after treadmill training (T) in WT mice (vs. *Myf5-Arl3*$^{-/-}$ mice). (*F*) The maximum distance was increased after treadmill training (T) in WT mice (vs. *Myf5-Arl3*$^{-/-}$ mice). Each dot represents the data from one mouse. (One-way ANOVA with Tukey's multiple comparisons tests, *$P < 0.05$, ***$P < 0.001$; NS, not significant.)

(*SI Appendix*, Fig. S5*B*). The results suggest that primary cilia are the mechanical sensors for *Pax7*-lineage myoblast differentiation in vitro.

These results suggested that the beneficial effects of mechanical stimulation on promoting myoblast differentiation are abrogated when SC cilia are dysfunctional.

The Induced Expression of Myogenic Gene Markers by Mechanical Stimulation Depends on Functional Primary Cilia. We extracted quadriceps muscle RNA from WT mice and *Myf5-Arl3*$^{-/-}$ mice and examined a panel of myogenic genes. We found the expression of myogenic markers (*MyoG*, *MyoD*, and *MyHC*) were not significantly different between WT, and *Myf5-Arl3*$^{-/-}$ mice (Fig. 4*A*). However, myogenic markers were induced in WT mice after 4-wk of treadmill training, but the induction was abrogated in *Myf5-Arl3*$^{-/-}$ mice (Fig. 4*B*). For in vitro analysis, the data show the expression of myogenic markers were induced in myoblasts derived from WT but not in those derived from *Myf5-Arl3*$^{-/-}$ mice (Fig. 4*C*). Similarly, the myogenic markers were induced with cyclic mechanical stretch stimulation in myoblasts derived from WT but not in those derived from *Myf5-Arl3*$^{-/-}$ mice (Fig. 4*D*). We also observed better induction of myogenic genes when myoblasts were cultured in serum-free medium (*SI Appendix*, Fig. S6*A*).

Induction of Hh Signaling Genes by Mechanical Stimulation Depends on Functional Primary Cilia. During skeletal muscle development, Hh signaling helps to initiate the myogenic program (22). When WT myoblasts are treated with Vismodegib, an Hh signaling inhibitor (35), we found that the induction of *MyoG*, *MyoD*, and *MyHC* expression was abrogated (Fig. 4*E*). To explore the effect of exercise on Hh signaling, we examined a panel of Hh signaling genes in RNA from WT mice and *Myf5-Arl3*$^{-/-}$ mice before and after exercise. We found that the induction of Hh signaling genes (*Gli1* and *Ptch1*) in WT mice after 4 wk of treadmill training was abrogated in *Myf5-Arl3*$^{-/-}$ mice (Fig. 5*A*). We also found that expression of the Hh signaling genes, *Gli1* and *Ptch1*, was increased in myoblasts derived from WT mice after mechanical stimulation but not in myoblasts derived from *Myf5-Arl3*$^{-/-}$ mice (Fig. 5*B*). Similarly, the Hh signaling genes were induced with cyclic mechanical stretch stimulation in myoblasts derived from WT but not in

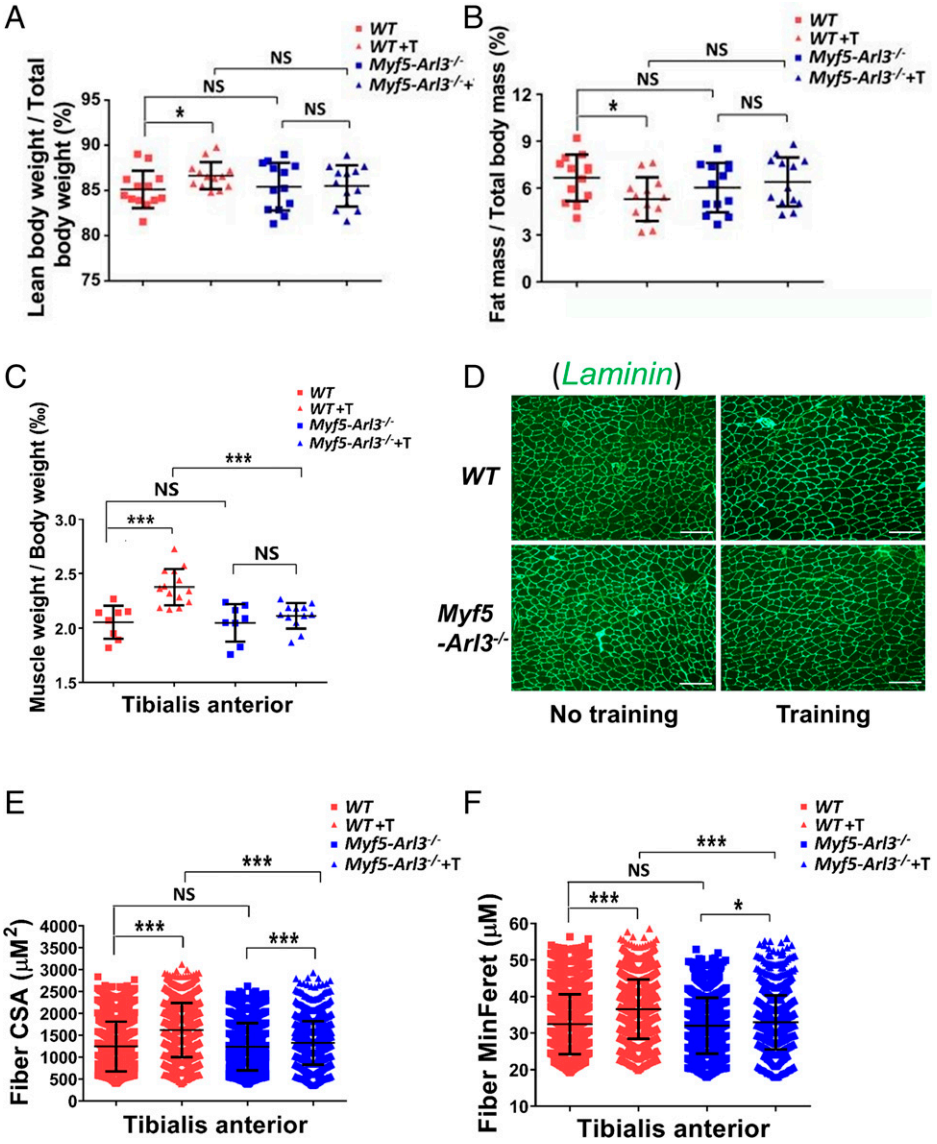

Fig. 2. Dysfunctional primary cilia impair exercise-induced muscle hypertrophy. (*A*) The ratio of lean bodyweight/total body weight ratio increased in WT mice after exercise, but not in the *Myf5-Arl3*$^{-/-}$ mice. (*B*) The ratio of fat mass/total body mass decreased in WT after exercise but not in *Myf5-Arl3*$^{-/-}$ mice. (*C*) The weights of TA were compared between WT and *Myf5-Arl3*$^{-/-}$ mice before and after treadmill training (T). (*D*) A representative image of TA stained by Laminin (green) is shown. (Scale bars, 100 μm.) (*E*) Fiber CSA of TA muscle fibers was determined using ImageJ and MyoVision software. (*F*) Fiber MinFere was quantified among TA muscle fibers using ImageJ and MyoVision software. NS, not significant. Each dot represents the data from one mouse. At least 3,000 fibers were measured for each sample. (One-way ANOVA with Tukey's multiple comparisons tests, **P* < 0.05, ****P* < 0.001; NS, not significant.)

those derived from *Myf5-Arl3*$^{-/-}$ mice (Fig. 5*C*). We also observed better induction of Hh signaling genes when myoblasts were cultured in serum-free medium (*SI Appendix*, Fig. S6*B*). When we treated WT myoblasts with Vismodegib, we found that the induction of *Gli1* and *Ptch1* was abolished (Fig. 5*D*).

When assessing whether mechanical stimulation promotes Hh target gene expression, we found that the percentage of ciliated myoblasts was not changed with mechanical stimulation (*SI Appendix*, Fig. S7). However, the length of primary cilia increased upon mechanical stimulation, and this elongation was abrogated in *Myf5-Arl3*$^{-/-}$ mice (Fig. 6 *A* and *B*). We also found that GLI3 translocated to cilia after mechanical stimulation in WT myoblasts, but not *Myf5-Arl3*$^{-/-}$ myoblasts, indicating the activation of the Hh signaling pathway with functional cilia (Fig. 6*C*). In addition, we treated myoblasts with Smoothened (SMO) Agonist (SAG), an agonist of the Hh signaling pathway, and found that SAG increased myogenic gene expression (Fig. 6*D*) and the Hh signaling pathway (Fig. 6*E*) in myoblasts derived from WT mice but not from *Myf5-Arl3*$^{-/-}$ mice.

We also examined the length of primary cilia upon mechanical stimulation in myoblasts isolated from *Pax7-Ift88*$^{-/-}$ mice and found the percentage of ciliated cells is significantly decreased in the *Pax7-Ift88*$^{-/-}$ myoblasts compared to WT myoblasts (*SI Appendix*, Fig. S8 *A* and *B*). We also found that elongation induced by mechanical stimulation was abrogated (*SI Appendix*, Fig. S8*C*). GLI3 translocated to cilia after mechanical stimulation in WT myoblasts, but not in *Pax7-Ift88*$^{-/-}$ myoblasts, indicating that the activation of the Hh signaling pathway requires functional cilia (*SI Appendix*, Fig. S8*D*).

Taken together, these results indicate that the Hh signaling pathway was activated by mechanical stimulation, and this activation depends predominately on functional cilia.

Conditioned Medium Treatment Analysis. To analyze if there are autocrine or paracrine of Hh ligands promoted by mechanical stimulation, we harvested conditioned medium on myoblasts after mechanical stimulation and analyzed with mass spectrometry analysis. We found no known Hh ligands in

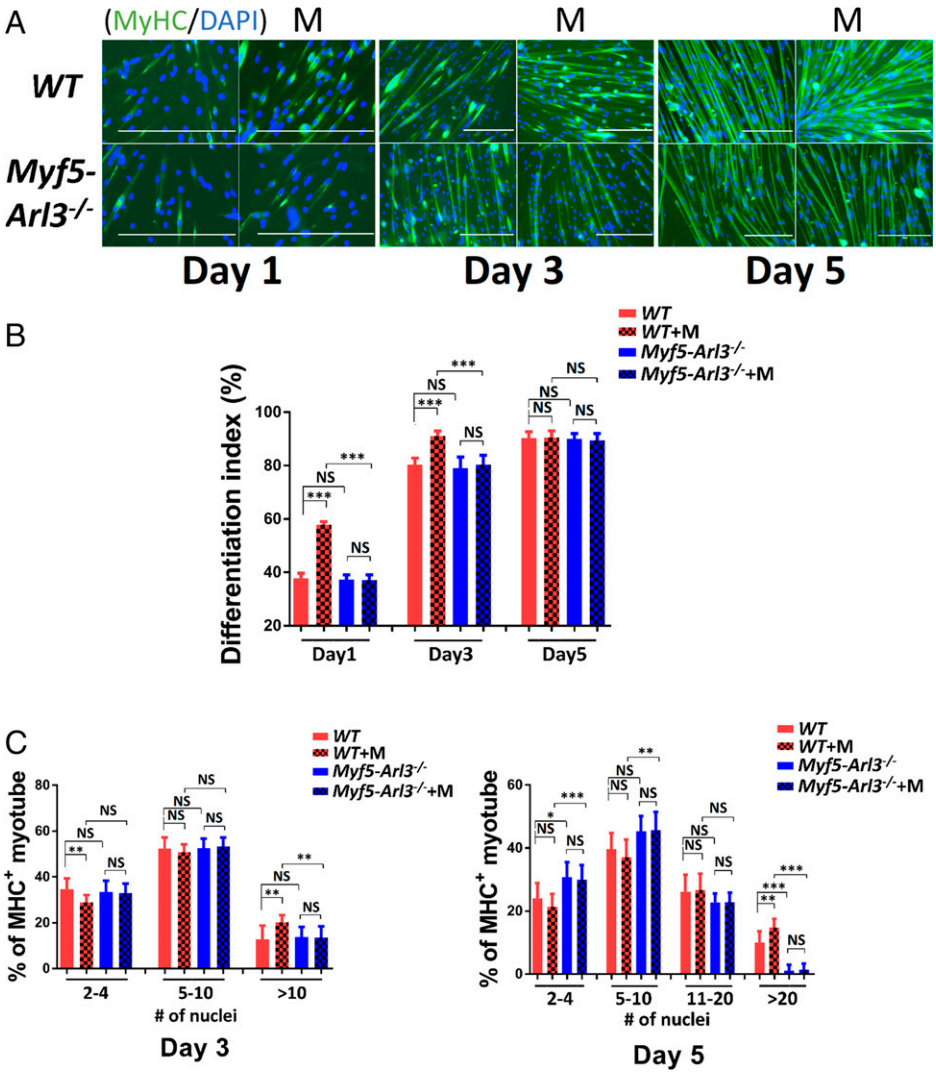

Fig. 3. Primary cilia are the mechanical sensors for myoblast differentiation in vitro. (*A*) MyHC (green) was stained at different days after mechanical stimulation (M) in myoblasts isolated from either WT or *Myf5-Arl3*$^{-/-}$ mice. (Scale bars, 100 μm.) (*B*) Differentiation index of myotubes (days 1, 3, and 5) were measured after mechanical stimulation in myoblasts. (*C*) Fusion index of myotubes (days 3 and 5) was measured after mechanical stimulation in myoblasts. Each sample represents the data from 1,000 myoblasts. (One-way ANOVA with Tukey's multiple comparisons tests, **P* < 0.05, ***P* < 0.01, ****P* < 0.001; NS, not significant.)

secretion protein after mass spectrometry experiments (Dataset S1). Then we treated the cells with the conditioned medium, and we did not find it can induce the activation of Hh (Fig. 5*E*). On the other hand, mechanical stimulation promotes Hh signaling in serum-free medium (*SI Appendix*, Fig. S6*B*). Taken together, our data support that mechanical stimulation itself can substitute for a Hh ligand.

Confirmation of the Abrogated Exercise Response in the *Pax7-Arl3*$^{-/-}$ Mouse Model. To confirm the abrogated exercise response in the cilium dysfunctional model, we bred *Pax7-Cre* lineage mice with *Arl3* floxed mice and obtained a grossly normal mouse model. When we trained 3-mo-old mice with forced exercise (treadmill testing at 10 m/min for 20 min, 5 d/wk for 4 wk), we found that the maximum speed and distance significantly increased in WT mice compared to *Pax7-Arl3*$^{-/-}$ mice (Fig. 7*A*). *Pax7-Arl3*$^{-/-}$ mice also increased their maximum speed (but not maximum distance) after exercise training (T),

We also found that mass from the TA, gastrocnemius, and vastus intermedius increased in WT mice but not in *Pax7-Arl3*$^{-/-}$ mice (Fig. 7*B*). We extracted quadriceps muscle RNA from WT mice and *Pax7-Arl3*$^{-/-}$ mice and examined a panel of myogenic genes. We found the expression of myogenic markers was induced in WT mice after 4-wk of treadmill training, but the induction was abrogated in *Pax7-Arl3*$^{-/-}$ mice (Fig. 7*C*). We found that the induction of Hh signaling genes (*Gli1* and *Ptch1*) in WT mice after 4 wk of treadmill training was abrogated in *Pax7-Arl3*$^{-/-}$ mice (Fig. 7*D*).

After staining the TA muscle with Laminin (Fig. 8*A*), we quantified myofibril size using the CSA and the minimal Feret's diameter of a muscle fiber cross-section. We found that exercise increased muscle fiber CSA in the TA from WT but not from *Pax7-Arl3*$^{-/-}$ mice (Fig. 8*B*). The exercise increased vastus intermedius and gastrocnemius muscle fiber CSA in both WT and *Pax7-Arl3*$^{-/-}$ mice, but *Pax7-Arl3*$^{-/-}$ mice exhibited less exercise-induced hypertrophy compared to WT mice (Fig. 8 *C* and *D*). These results indicate that the increased muscle fiber CSA due to the mechanical stimulation of exercise largely depends on functional cilia.

Discussion

Primary cilia are nonmotile, solitary, antenna-like structures that protrude from the surface of cells. Concentrating critical

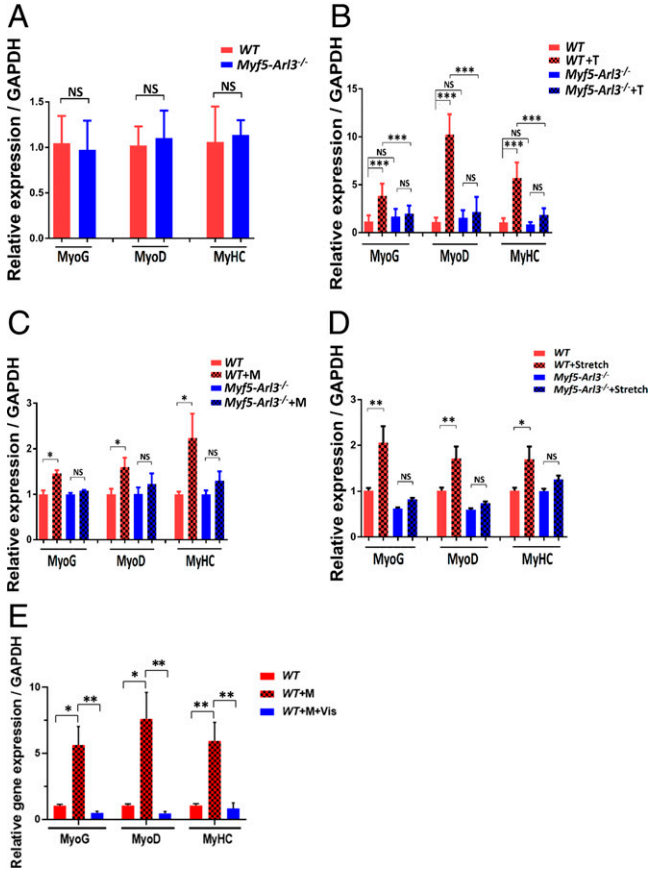

Fig. 4. The induced expression of myogenic gene markers by mechanical stimulation and exercise depends on functional primary cilia. (*A*) Relative expression of *MyoG*, *MyoD*, and *MyHC* expression in TA from WT and *Myf5-Arl3*$^{-/-}$ mice at the age of 1 mo using a real-time PCR test. (*B*) Relative expression of *MyoG*, *MyoD*, and *MyHC* expression in TA in *Myf5-Arl3*$^{-/-}$ mice after treadmill training (T) in vivo using a real-time PCR test. (*C*) Relative expression of *MyoG*, *MyoD*, and *MyHC* in *Myf5-Arl3*$^{-/-}$ myoblasts after mechanical stimulation (M) in vitro using real-time PCR. (*D*) The relative expression of *MyoG*, *MyoD*, and *MyHC* expression in myoblasts derived from WT and *Myf5-Arl3*$^{-/-}$ mice with cyclic mechanical stretch (Stretch) stimulation. (*E*) Relative *MyoG*, *MyoD*, and *MyHC* expression in myoblasts derived from WT mice and treated with or without Vismodegib (Vis). (One-way ANOVA with Tukey's multiple comparisons tests, **P* < 0.05, ***P* < 0.01, ****P* < 0.001; NS, not significant.)

signaling components in a tiny ciliary volume amplifies responses to low levels of environmental cues (36, 37). However, it is unclear if primary cilia sense mechanical force as well as the physiological importance of SC cilia in exercise-induced muscle hypertrophy. Identifying the molecular sensors of mechanical stimulation and underlying signaling pathways will substantially impact the future design of exercise interventions.

The primary intervention to improve muscle strength and to minimize muscle atrophy continues to be weight-bearing and other exercises. Almost all studies that employed an exercise intervention only addressed functional and health outcomes (38). To our knowledge, no studies have described how extracellular mechanical signals are transduced to myoblasts and regulate responsive gene expression to affect muscle hypertrophy. Our data demonstrate that exercise increased the maximum speed/distance after treadmill training and promoted muscle hypertrophy and myogenic gene expression in WT but not *Myf5-Arl3*$^{-/-}$ and *Pax7-Arl3*$^{-/-}$ mice. We also confirmed that mechanical stimulation promoted myoblast differentiation in WT myoblasts but was diminished in *Myf5-Arl3*$^{-/-}$ and *Pax7-Ift88*$^{-/-}$ myoblasts. We further showed that the Hh signaling pathway is induced by mechanical stimulation in vitro and exercise in vivo. The induction was abrogated if cilia in SCs are dysfunctional. We provide evidence for the proof-of-concept that cilia in SCs are mechanical sensors in exercise and mechanical stimulation.

Myf5-Arl3$^{-/-}$ mice show "normal" development but loss of the response to exercise-induced hypertrophy in mice, even if there is, maybe, a minor delay in the development of mutants. However, this could be very interesting because it suggested that the two processes might be regulated by different progenitor cells. This will also highlight that targeting SC cilia could be safe since it won't affect normal muscle generation. The observations that mechanical stimulation can activate the Hh signaling pathway suggest that mechanical stimulation can be sensed directly by cilia in a ligand-independent way or with only trace amounts of ligands. A schematic illustrating of mechanical stimulation activating Hh signaling in the primary cilium is shown (Fig. 9*A*).

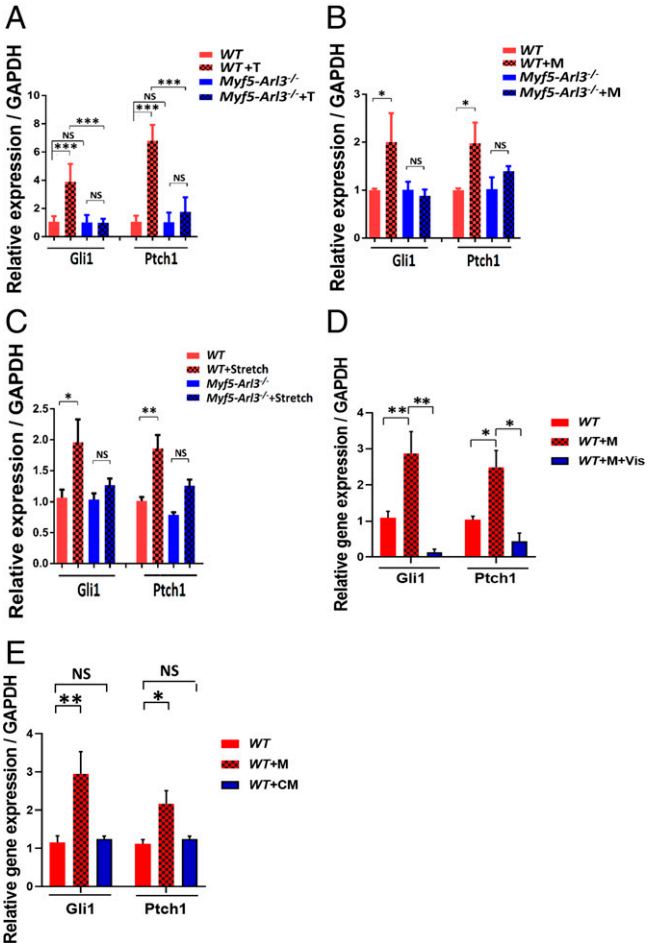

Fig. 5. Abrogated induction of Hh signaling markers in *Myf5-Arl3*$^{-/-}$ mice after treadmill training (T), mechanical stimulation, and stretch. (*A*) Relative expression of *Gli1* and *Ptch1* expression in TA in *Myf5-Arl3*$^{-/-}$ mice after treadmill training (T). (*B*) Relative expression of *Gli1* and *Ptch1* in myoblasts derived from WT and *Myf5-Arl3*$^{-/-}$ mice after mechanical stimulation (M) in vitro using real-time PCR. (*C*) Relative expression of *Gli1* and *Ptch1* in myoblasts derived from WT and *Myf5-Arl3*$^{-/-}$ mice after cyclic mechanical stretch (Stretch) stimulation in vitro using real-time PCR. (*D*) Real-time PCR analysis of *Gli1* and *Ptch1* expression in myoblasts derived from WT mice and treated with or without Vismodegib (Vis). (*E*) Real-time PCR analysis of *Gli1* and *Ptch1* expression in myoblasts derived from WT mice and treated with conditioned medium (CM). (One-way ANOVA with Tukey's multiple comparisons tests, **P* < 0.05, ***P* < 0.01, ****P* < 0.001; NS, not significant.)

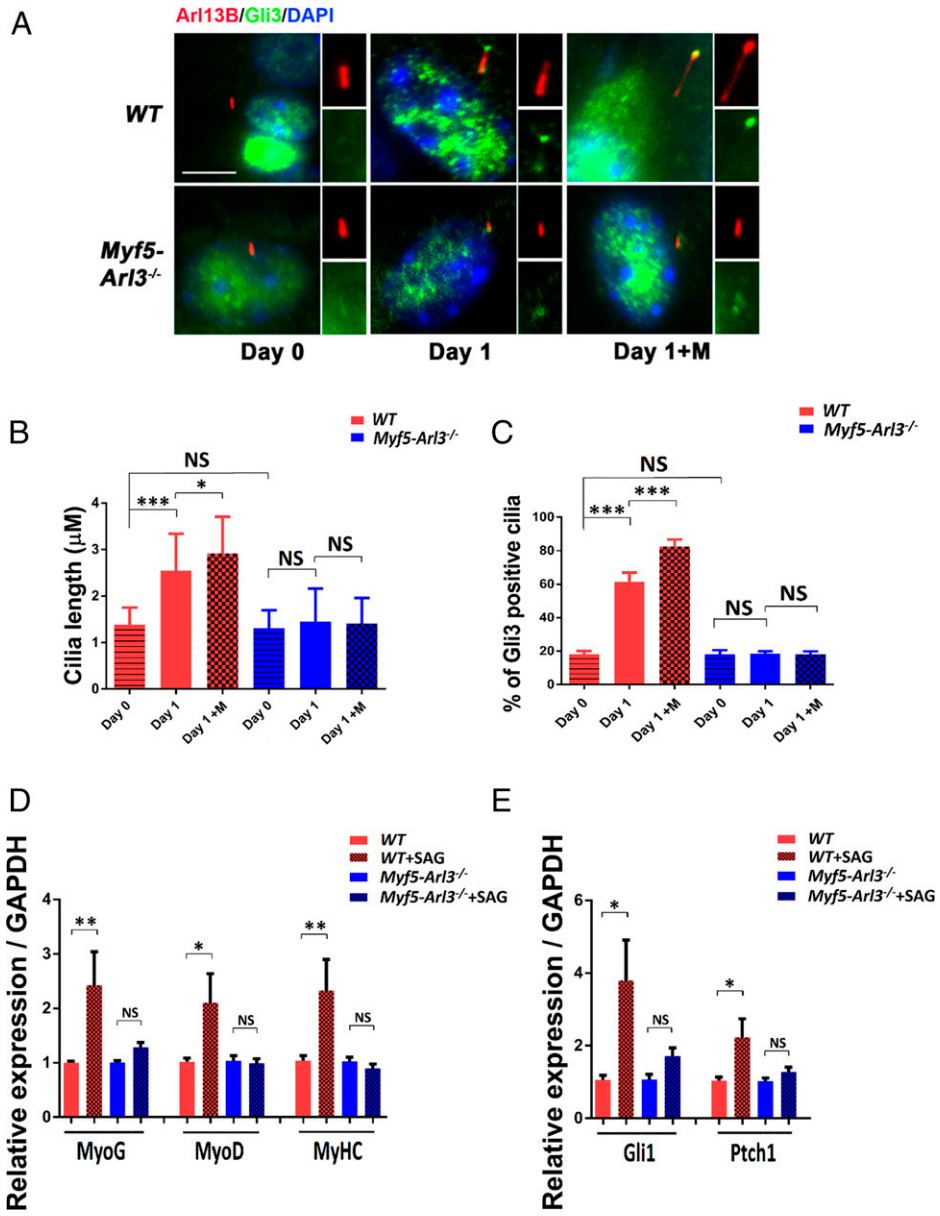

Fig. 6. The activation of the Hh signaling pathway by mechanical stimulation depends on functional primary cilia. (*A*) GLI3 translocates to cilia after mechanical stimulation in WT but not *Myf5-Arl3*$^{-/-}$ myoblasts. Immunofluorescence staining of cilia with ARL13B (red) and GLI3 (green) and counterstained with DAPI (blue). GLI3^{+} cilia were counted. (Scale bar, 5 μm.) (*B*) The length of cilia was measured using a Nikon ECLIPSE Ti with MetaMorph software. An average of 300 cilia was measured in each group. (*C*) Quantification of *A*: 300 cells were counted for each line (five lines for each genotype). (*D*) Relative expression of *MyoG*, *MyoD*, and *MyHC* in myoblasts derived from WT and *Myf5-Arl3*$^{-/-}$ mice after SAG treatment using real-time PCR. (*E*) Relative expression of *Gli1* and *Ptch1* expression in myoblasts derived from WT and *Myf5-Arl3*$^{-/-}$ mice after SAG treatment using real-time PCR. Note the abrogation of Hh signaling markers in *Myf5-Arl3*$^{-/-}$ mice after mechanical stimulation in vitro. (One-way ANOVA with Tukey's multiple comparisons tests, $*P < 0.05$, $**P < 0.01$, $***P < 0.001$; NS, not significant.)

We also tried to establish the *Pax7*-specific *Ift88* conditional knockout mouse model. However, the *Pax7-Ift88*$^{-/-}$ mice developed hydrocephalus and could not support their weight by the age of 3 wk. After examining myoblasts from *Pax7-Ift88*$^{-/-}$ mice, we found that the response to mechanical stimulation was abrogated. Due to the coexpression of *Pax7* and *Myf5* in the majority of myoblasts and the crucial function of Arl3 and Ift88 in cilia, it is not surprising we observed a similar response in myoblasts derived from *Pax7-Ift88*$^{-/-}$ and *Myf5-Arl3*$^{-/-}$ mice. It is also not surprising that we observed a similar response between *Pax7-Arl3*$^{-/-}$ and *Myf5-Arl3*$^{-/-}$ mice.

We propose that the ciliary-Hh signaling pathway is the primary pathway responsible for sensing mechanical stimulation in myoblasts. However, we cannot exclude other signaling molecules. Cilia harbor a calcium-channel protein that is thought to open when the cilium is bent by the force of fluid flow, allowing calcium ions (Ca^{2+}) to enter the cell (39–41). Consistently, several mechanosensitive ion channels, such as Polycystins, TRPV4 (transient receptor potential channel vanilloid subfamily 4), and PIEZO1 (piezo-type mechanosensitive ion channel component 1) have been implicated in the context of mammalian cilia (20, 42–44). It is thus likely mechanical stimulation promotes an increase in cytosolic calcium concentration ($[Ca^{2+}]_{cyt}$) in myoblasts or that calcium and Hh signaling are not mutually exclusive. Further investigation can clarify the link between Hh signaling, the regulation of $[Ca^{2+}]_{cyt}$, and mechanical stimulation in SCs. Moreover, nitric oxide (NO), a key regulator of homeostasis and adaptive responses of the vascular system, generated by NO

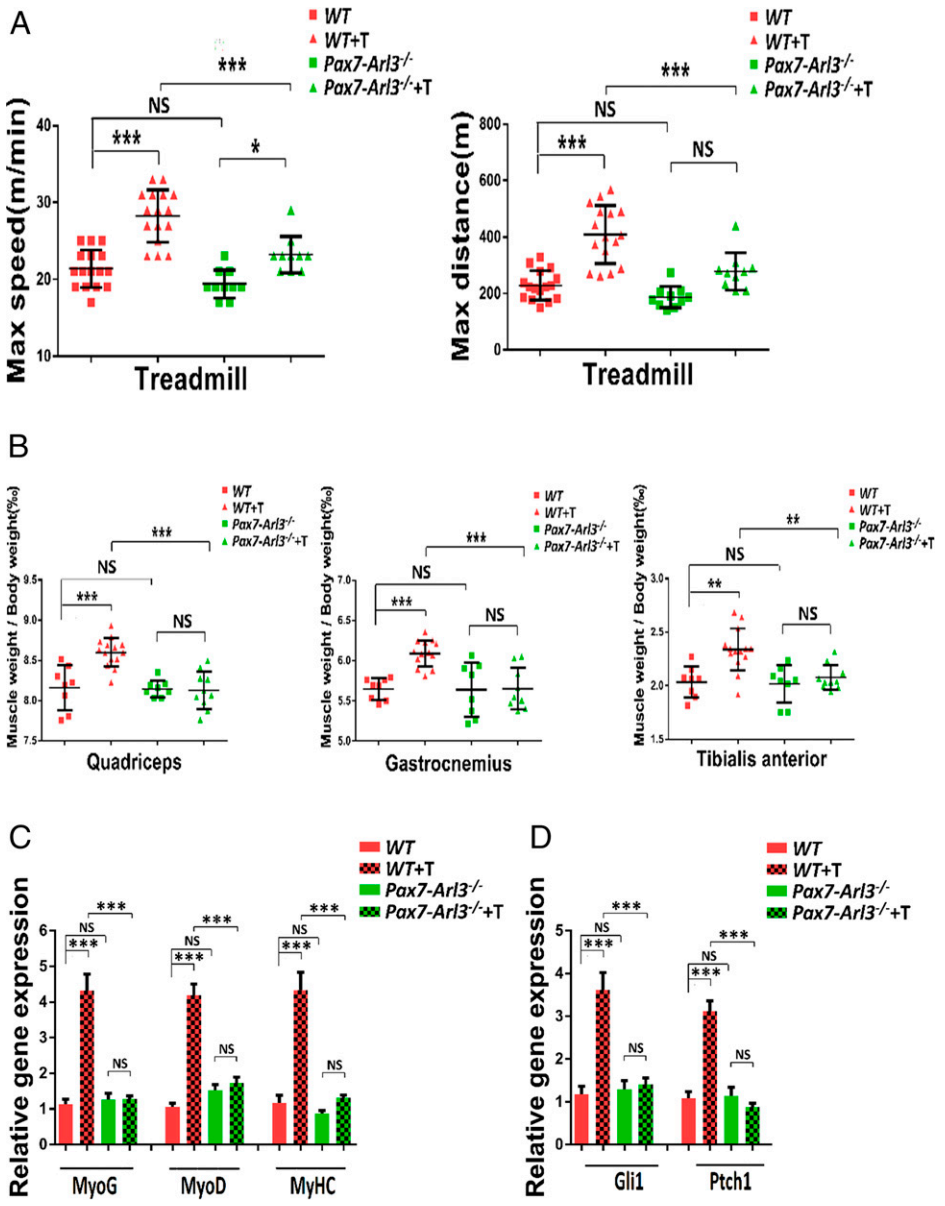

Fig. 7. The characterization of *Pax7-Arl3*$^{-/-}$ mouse model. (*A*) The maximum distance was increased after treadmill training (T) in WT mice (vs. *Pax7-Arl3*$^{-/-}$ mice). (*B*) The weights of quadriceps, gastrocnemius, and TA were compared between WT and *Pax7-Arl3*$^{-/-}$ mice before and after treadmill training (T). (*C*) Relative expression of *MyoG*, *MyoD*, and *MyHC* expression in TA in *Pax7-Arl3*$^{-/-}$ mice after treadmill training (T) in vivo using real-time PCR test. (*D*) Relative expression of *Gli1* and *Ptch1* expression in TA in *Pax7-Arl3*$^{-/-}$ mice after treadmill training (T). Each dot represents the data from one mouse. (One-way ANOVA with Tukey's multiple comparisons tests, **P* < 0.05, ***P* < 0.01, ****P* < 0.001; NS, not significant.)

synthases (NOS), may also play a role in transducing mechanical stimulation (45). The main NOS isoform in endothelial cells is eNOS and cyclic stretch is an important inducer of eNOS expression and activity (46).

In addition, circulating mediators are known to play a significant role in regulating muscle regeneration (47). However, we did not observe that conditioned medium promotes the activation of the Hh-signaling pathway in myoblasts. The Hh signaling pathway is one of the most important signaling pathways involved in development and tissue homeostasis (48). Our data suggest that mechanical stimulation itself likely substitutes for Hh ligands, or may strengthen the signal of residual Hh ligands that could not be detected by our analysis, to activate Hh response in cilia-dependent manner. Moreover, other signaling pathways that cross-talk with Hh signaling may be involved. Further investigation on different signaling pathways is highly suggested.

Ligand-independent Hh signaling is associated with a subset of human tumors, such as basal cell carcinoma, medulloblastoma, colorectal, breast, and so forth (49). The deletion of mutation in Ptch1 and SMO in tumors results in ligand-independent constitutive Hh pathway activation. Our findings in SC that ligand-independent Hh signaling may be significant for the understanding of the supportive microenvironment for tumor growth.

In summary, we provide proof-of-concept evidence that primary cilia in SCs are the mechanical sensors for muscle hypertrophy. In general, exercise exerts benefits on body composition for many people. Some individuals quickly adapt to exercise, build up muscle mass, and reduce body fat (50, 51). However, other individuals are resistant to exercise (52). Identifying the mechanical sensors in skeletal muscle and their mechanisms of signal transduction will decipher a fundamental physiological problem to explain why some people are exercise-resistant (Fig.

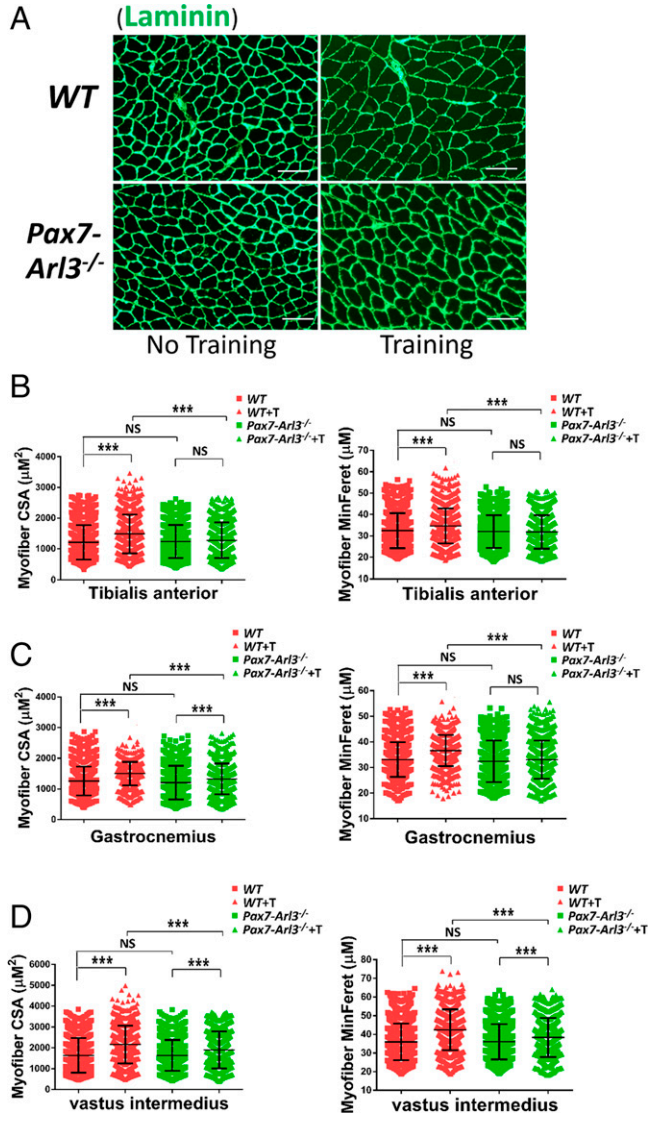

Fig. 8. Dysfunctional primary cilia impair exercise-induced muscle hypertrophy in *Pax7-Arl3*$^{-/-}$ mice. (*A*) Gastrocnemius muscle fiber CSA was quantified using ImageJ and MyoVision software. (Scale bars, 50 μm.) (*B*) Fiber MinFere was quantified for muscle fibers from the gastrocnemius using ImageJ and MyoVision software. (*C*) Vastus intermedius muscle fiber CSA was quantified using ImageJ and MyoVision software. (*D*) Fiber MinFere was quantified for muscle fibers from the TA using ImageJ and MyoVision software. Each dot represents the data from one mouse. NS, not significant. At least 3,000 fibers were measured for each sample. (One-way ANOVA with Tukey's multiple comparisons tests, ***$P < 0.001$; NS, not significant.)

9*B*). Clarifying the responsive molecular events will provide possible molecular targets for the prevention or amelioration of muscle atrophy due to physical disability, coma, paralysis, or improve the effects of exercise in those who are less responsive to it.

Materials and Methods

Cell Models. Primary mouse myoblasts were isolated based on a previously published method (53). At the age of 2 to 3 wk, WT and *Myf5-Arl3*$^{-/-}$ mice were killed, the hind limb muscles were isolated, and excess connective tissues and fat were cleaned in sterile PBS. Muscle tissues were then minced into small pieces, followed by culture on a 10% Matrigel-coated dish with growth medium (high-glucose DMEM [Gibco], supplemented with 20% fetal bovine serum, [Gibco], 0.5% chicken embryo extract [CEE, Accurate Chemical and Scientific], 2.5 ng/mL basic fibroblast growth factor [bFGF, PeproTech], and 1% penicillin–streptomycin). After outgrowth from muscle explants was observed, muscle tissues were removed and cells were grown to confluence. For serial cultivation, cells were preplated on a non-Matrigel–coated dish and placed at 37 °C in a CO_2 incubator for 1 h. Then the supernatant was transferred to a 10% Matrigel-coated dish for the first five passages to select for a pure myoblast population. The isolated myoblasts were grown on Matrigel-coated dishes with 20% serum, CEE, and FGF.

Human skeletal muscle myoblasts primary cell strains from different donors of similar ages were obtained from Lonza and propagated using a growth medium purchased from Lonza and cultured following the company's standard protocol.

Animal Models. WT mice (C57BL/6J) and *Myf5* cre mice are from the Jackson Laboratory. The *Arl3* floxed mice were established by Wolfgang Baehr's laboratory, University of Utah, Salt Lake City, UT (12). *Myf5-Arl3*$^{-/-}$ mice were obtained from breeding *Myf5* cre mice and *Arl3* floxed mice. *Pax7* cre [Pax7tm1(cre) Mrc/J] mice and Ift88 (B6.129P2-Ift88tm1Bky/J) mice are from the Jackson Laboratory (54). *Pax7-Ift88*$^{-/-}$ mice were obtained from breeding *Pax7*-cre mice and *Ift88*-floxed mice. *Pax7-Arl3*$^{-/-}$ mice were obtained from breeding *Pax7*-cre mice and *Arl3*- floxed mice. An equal number of male and female mice were assessed. All mice were confirmed by genotyping. All experimental protocols with mice were approved in advance by the Institutional Animal Care and Use Committee and Institutional Biosafety Committee at the Mayo Clinic.

Treadmill Testing. Physical function was characterized by measuring running time and distance using a motorized, inclined treadmill. Mice were acclimated to the treadmill for 3 consecutive days for 5 min at a speed of 10 m/min at a 5% grade. The next day animals ran on the treadmill at an initial speed of 10 m/min and 5% grade for 4 min, and every additional 4 min the speed was increased by 2 m/min until the mice were exhausted. Running time was recorded and running distance and work (the product of body weight [kg], gravity [9.81 m/s^2], vertical speed [m/s × angle], and time [s]) were calculated.

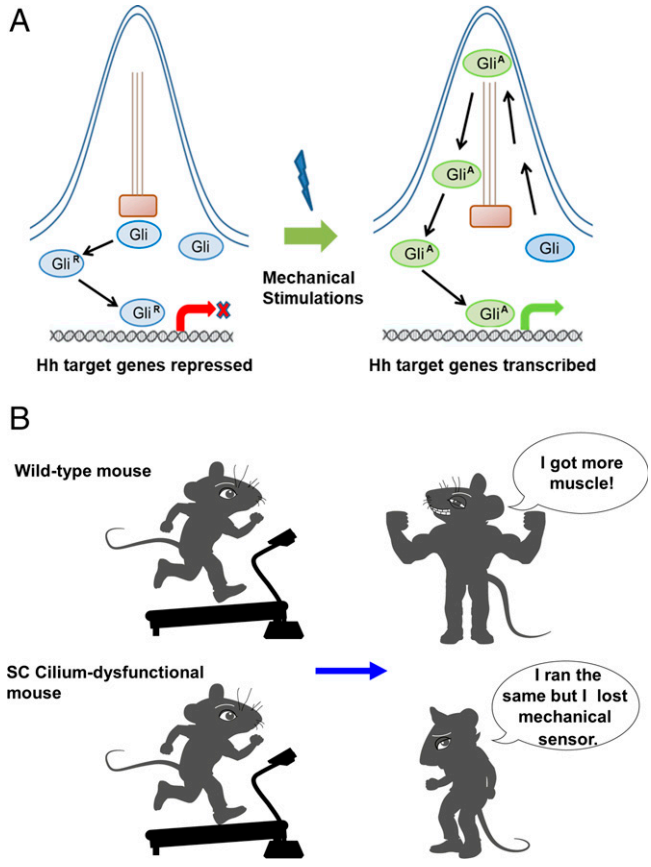

Fig. 9. A schematic illustrating how mechanical stimulation activates Hh signaling in the primary cilium. (*A*) In the absence of mechanical stimulation, cilia do not activate nuclear GLI activity. In the presence of mechanical stimulation, the nuclear GLI activity activates the downstream targets of the Hh signaling pathway. (*B*) A cartoon indicates WT mice can build up muscle. However, SC cilium-dysfunctional mice show exercise resistance.

Analysis of Muscle Hypertrophy. For imaging analysis, TA was fixed and embedded in an optimum cutting temperature compound (Sakura Finetek) and snap-frozen in liquid nitrogen-cooled isopentane. Muscles were cryosectioned at 10 μm at midbelly. Randomly selected images across all sections were used for histology. The muscle structure was analyzed by H&E staining and histomorphometry, and the basement membranes surrounding the myofibrils were stained with laminin antibodies (Sigma). The CSA of muscle fibers was analyzed with ImageJ and MyoVision software (developed by the Center for Muscle Biology, University of Kentucky).

Mechanical Induction of Myoblast Differentiation. For each cell strain, cells were seeded and grown to confluence. Half of the cells were treated with mechanical stimulation on Dynamic Motion Platform for 10 min every day or mechanical stretch for 1 h every day as the experimental group, and half of the cells were untreated as the control group. At each time point (days 1, 3, and 5), MyHC immunofluorescence staining and myoblast fusion index were measured, and RNA expression of *MyoG*, *MyoD*, and *MyHC* was examined.

Differentiation and Fusion Assays. Myoblasts were maintained in growth medium until reaching ∼70% confluency and then seeded onto 10% Matrigel-coated six-well plates in Growth Medium until reaching confluency. Myoblasts were then switched to differentiation medium (DM) (DMEM [Gibco] supplemented with 2% horse serum). For the serum-free experiment (*SI Appendix*, Fig. S6), myoblasts were cultured with DMEM only. Cultured myoblasts were fixed for 15 min in 4% PFA after 1, 3, or 5 d in DM, rinsed in PBS and PBS-T (0.2% Triton X-100 in PBS), and processed for immunofluorescence. The differentiation index was defined as the percentage of nuclei in myosin$^+$ cells. The fusion index was calculated as the percentage of nuclei in the myotubes. More than 100 MyHC$^+$ myotubes containing two or more nuclei were counted to measure fusion efficiency. More than five field images (20× objective) were analyzed per experimental group. The results presented are from four to five independent experiments. Image parameters were equally adjusted using Photoshop CS6 software (Adobe).

SAG and Vismodegib Treatment Analysis. Myoblasts were seeded onto 10% Matrigel-coated six-well plates in growth medium until reaching confluency. After 24-h starvation, myoblasts were treated with 200 μM SAG (R&D Company) or 1 μM Vismodegib (ThermoFisher) in DMEM serum-free medium. After 24 h, total RNA was collected and the expression of *MyoG*, *MyoD*, *MyHC*, *Gli1*, and *Ptch1* was compared by real-time PCR.

Mechanical Stimulation-Conditioned Medium Treatment Analysis. WT myoblasts were seeded onto 10% Matrigel-coated six-well plates in a growth medium until reaching confluency. After 24-h starvation, myoblasts were treated with mechanical stimulation in DMEM serum-free medium. After another 24 h, a portion of the supernatant was collected for mass spectrometry of protein and peptides analysis, and a portion of the supernatant was used to treat the myoblasts for 24 h. The expression of *Gli1* and *Ptch1* was compared by real-time PCR.

Bodyweight and Body Composition. Bodyweight was measured every week. The lean mass and fat mass of individual mice was measured by quantitative NMR using an EchoMRI analyzer (EchoMRI) and normalized to body weight.

Cilia Length Measurement. The length of cilia was measured using a Nikon ECLIPSE Ti with MetaMorph software (Molecular Devices). An average of 300 cilia was measured in each group.

Statistical Analyses. All experiments were performed with at least three technical and biological replicates unless otherwise indicated in the figure legends. Data were checked for normality using histograms, and all variables were tested for skewness and kurtosis. The key primary comparisons were between exercise or mechanical stimulation and control samples using a one-way ANOVA with mechanical treatment or exercise as an independent variable with a significance level of 0.05. Following ANOVA, Tukey's test was used to adjust for multiple comparisons. Data were represented as mean ± SEM.

Data Availability. All study data are included in the main text and supporting information.

ACKNOWLEDGMENTS. We thank Dr. Beyder Arthur of the Mayo Clinic for help on the Cyclic Mechanical Stretch Platform; and Wolfgang Baehr from the University of Utah for the gift of the *Arl3* mouse model. This work was supported in part by the Center for Clinical and Translational Science at the Mayo Clinic (H.W.), The Center for Biomedical Discovery at Mayo Clinic (H.W. and J.H.), and the Robert and Arlene Kogod Professorship in Geriatric Medicine (R.J.P.).

1. C. Bouchard, T. Rankinen, J. A. Timmons, Genomics and genetics in the biology of adaptation to exercise. *Compr. Physiol.* **1**, 1603–1648 (2011).
2. H. Misu *et al.*, Deficiency of the hepatokine selenoprotein P increases responsiveness to exercise in mice through upregulation of reactive oxygen species and AMP-activated protein kinase in muscle. *Nat. Med.* **23**, 508–516 (2017).
3. C. Bouchard *et al.*, Familial aggregation of VO(2max) response to exercise training: Results from the HERITAGE Family Study. *J. Appl. Physiol.* **87**, 1003–1008 (1999).
4. S. Hody, J. L. Croisier, T. Bury, B. Rogister, P. Leprince, Eccentric muscle contractions: Risks and benefits. *Front. Physiol.* **10**, 536 (2019).
5. N. A. Stephens, L. M. Sparks, Resistance to the beneficial effects of exercise in type 2 diabetes: Are some individuals programmed to fail? *J. Clin. Endocrinol. Metab.* **100**, 43–52 (2015).
6. D. Holmes, Metabolism: Exercise resistance decoded. *Nat. Rev. Endocrinol.* **13**, 251 (2017).
7. M. Spasic, C. R. Jacobs, Lengthening primary cilia enhances cellular mechanosensitivity. *Eur. Cell. Mater.* **33**, 158–168 (2017).
8. T. R. Coughlin *et al.*, Primary cilia expression in bone marrow in response to mechanical stimulation in explant bioreactor culture. *Eur. Cell. Mater.* **32**, 111–122 (2016).
9. J. Wu *et al.*, Characterization of primary cilia in human airway smooth muscle cells. *Chest* **136**, 561–570 (2009).
10. G. Novarino, N. Akizu, J. G. Gleeson, Modeling human disease in humans: The ciliopathies. *Cell* **147**, 70–79 (2011).
11. M. Lokaj *et al.*, The interaction of CCDC104/BARTL1 with Arl3 and implications for ciliary function. *Structure* **23**, 2122–2132 (2015).
12. C. Hanke-Gogokhia *et al.*, Arf-like protein 3 (ARL3) regulates protein trafficking and ciliogenesis in mouse photoreceptors. *J. Biol. Chem.* **291**, 7142–7155 (2016).
13. S. R. Bhattarai, S. Begum, R. Popow, E. J. Ezratty, The ciliary GTPase Arl3 maintains tissue architecture by directing planar spindle orientation during epidermal morphogenesis. *Development* **146**, dev161885 (2019).
14. S. Alkanderi *et al.*, ARL3 mutations cause joubert syndrome by disrupting ciliary protein composition. *Am. J. Hum. Genet.* **103**, 612–620 (2018).
15. R. De Mori *et al.*, Hypomorphic recessive variants in SUFU impair the sonic hedgehog pathway and cause Joubert syndrome with cranio-facial and skeletal defects. *Am. J. Hum. Genet.* **101**, 552–563 (2017).
16. H. Kim *et al.*, Ciliary membrane proteins traffic through the Golgi via a Rabep1/GGA1/Arl3-dependent mechanism. *Nat. Commun.* **5**, 5482 (2014).
17. H. A. Praetorius, K. R. Spring, Bending the MDCK cell primary cilium increases intracellular calcium. *J. Membr. Biol.* **184**, 71–79 (2001).
18. H. A. Praetorius, K. R. Spring, Removal of the MDCK cell primary cilium abolishes flow sensing. *J. Membr. Biol.* **191**, 69–76 (2003).
19. H. A. Praetorius, K. R. Spring, The renal cell primary cilium functions as a flow sensor. *Curr. Opin. Nephrol. Hypertens.* **12**, 517–520 (2003).
20. S. M. Nauli *et al.*, Polycystins 1 and 2 mediate mechanosensation in the primary cilium of kidney cells. *Nat. Genet.* **33**, 129–137 (2003).
21. G. J. Pazour, G. B. Witman, The vertebrate primary cilium is a sensory organelle. *Curr. Opin. Cell Biol.* **15**, 105–110 (2003).
22. S. C. Goetz, K. V. Anderson, The primary cilium: A signalling centre during vertebrate development. *Nat. Rev. Genet.* **11**, 331–344 (2010).
23. W. Fu, P. Asp, B. Canter, B. D. Dynlacht, Primary cilia control hedgehog signaling during muscle differentiation and are deregulated in rhabdomyosarcoma. *Proc. Natl. Acad. Sci. U.S.A.* **111**, 9151–9156 (2014).
24. D. Kopinke, E. C. Roberson, J. F. Reiter, Ciliary hedgehog signaling restricts injury-induced adipogenesis. *Cell* **170**, 340–351.e12 (2017).
25. B. Bazgir, R. Fathi, M. Rezazadeh Valojerdi, P. Mozdziak, A. Asgari, Satellite cells contribution to exercise mediated muscle hypertrophy and repair. *Cell J.* **18**, 473–484 (2017).
26. C. S. Fry *et al.*, Regulation of the muscle fiber microenvironment by activated satellite cells during hypertrophy. *FASEB J.* **28**, 1654–1665 (2014).
27. K. A. Murach *et al.*, Differential requirement for satellite cells during overload-induced muscle hypertrophy in growing versus mature mice. *Skelet. Muscle* **7**, 14 (2017).
28. D. M. Frechette, D. Krishnamoorthy, B. J. Adler, M. E. Chan, C. T. Rubin, Diminished satellite cells and elevated adipogenic gene expression in muscle as caused by ovariectomy are averted by low-magnitude mechanical signals. *J. Appl. Physiol.* **119**, 27–36 (2015).
29. G. Ceccarelli *et al.*, Low-amplitude high frequency vibration down-regulates myostatin and atrogin-1 expression, two components of the atrophy pathway in muscle cells. *J. Tissue Eng. Regen. Med.* **8**, 396–406 (2014).
30. S. Kuang, K. Kuroda, F. Le Grand, M. A. Rudnicki, Asymmetric self-renewal and commitment of satellite stem cells in muscle. *Cell* **129**, 999–1010 (2007).
31. S. Günther *et al.*, Myf5-positive satellite cells contribute to Pax7-dependent long-term maintenance of adult muscle stem cells. *Cell Stem Cell* **13**, 590–601 (2013).
32. J. von Maltzahn, A. E. Jones, R. J. Parks, M. A. Rudnicki, Pax7 is critical for the normal function of satellite cells in adult skeletal muscle. *Proc. Natl. Acad. Sci. U.S.A.* **110**, 16474–16479 (2013).
33. F. Relaix, D. Rocancourt, A. Mansouri, M. Buckingham, A Pax3/Pax7-dependent population of skeletal muscle progenitor cells. *Nature* **435**, 948–953 (2005).
34. G. Parise, I. W. McKinnell, M. A. Rudnicki, Muscle satellite cell and atypical myogenic progenitor response following exercise. *Muscle Nerve* **37**, 611–619 (2008).
35. N. H. Jaafar Marican, S. B. Cruz-Migoni, A. G. Borycki, Asymmetric distribution of primary cilia allocates satellite cells for self-renewal. *Stem Cell Reports* **6**, 798–805 (2016).

36. E. S. Seeley, M. V. Nachury, The perennial organelle: Assembly and disassembly of the primary cilium. *J. Cell Sci.* **123**, 511–518 (2010).
37. I. Sánchez, B. D. Dynlacht, Cilium assembly and disassembly. *Nat. Cell Biol.* **18**, 711–717 (2016).
38. D. Bishop-Bailey, Mechanisms governing the health and performance benefits of exercise. *Br. J. Pharmacol.* **170**, 1153–1166 (2013).
39. Y. Iwadate, Y. Nakaoka, Calcium regulates independently ciliary beat and cell contraction in Paramecium cells. *Cell Calcium* **44**, 169–179 (2008).
40. S. M. Nauli, R. Pala, S. J. Kleene, Calcium channels in primary cilia. *Curr. Opin. Nephrol. Hypertens.* **25**, 452–458 (2016).
41. D. P. Norris, P. K. Jackson, Cell biology: Calcium contradictions in cilia. *Nature* **531**, 582–583 (2016).
42. A. Miyazaki *et al.*, Coordination of WNT signaling and ciliogenesis during odontogenesis by piezo type mechanosensitive ion channel component 1. *Sci. Rep.* **9**, 14762 (2019).
43. K. L. Lee *et al.*, The primary cilium functions as a mechanical and calcium signaling nexus. *Cilia* **4**, 7 (2015).
44. N. Luo *et al.*, Primary cilia signaling mediates intraocular pressure sensation. *Proc. Natl. Acad. Sci. U.S.A.* **111**, 12871–12876 (2014).
45. K. Ghimire *et al.*, MAGI1 mediates eNOS activation and NO production in endothelial cells in response to fluid shear stress. *Cells* **8**, 388 (2019).
46. M. A. Corson *et al.*, Phosphorylation of endothelial nitric oxide synthase in response to fluid shear stress. *Circ. Res.* **79**, 984–991 (1996).
47. S. A. Beckman *et al.*, Beneficial effect of mechanical stimulation on the regenerative potential of muscle-derived stem cells is lost by inhibiting vascular endothelial growth factor. *Arterioscler. Thromb. Vasc. Biol.* **33**, 2004–2012 (2013).
48. J. Zhang, Z. Liu, J. Jia, Mechanisms of smoothened regulation in hedgehog signaling. *Cells* **10**, 2138 (2021).
49. S. Teglund, R. Toftgård, Hedgehog beyond medulloblastoma and basal cell carcinoma. *Biochim. Biophys. Acta* **1805**, 181–208 (2010).
50. K. R. Westerterp, Exercise, energy balance and body composition. *Eur. J. Clin. Nutr.* **72**, 1246–1250 (2018).
51. K. Liberman, L. N. Forti, I. Beyer, I. Bautmans, The effects of exercise on muscle strength, body composition, physical functioning and the inflammatory profile of older adults: A systematic review. *Curr. Opin. Clin. Nutr. Metab. Care* **20**, 30–53 (2017).
52. J. Bidonde *et al.*, Aerobic exercise training for adults with fibromyalgia. *Cochrane Database Syst. Rev.* **6**, CD012700 (2017).
53. A. Shahini *et al.*, Efficient and high yield isolation of myoblasts from skeletal muscle. *Stem Cell Res. (Amst.)* **30**, 122–129 (2018).
54. M. D. Tallquist, K. E. Weismann, M. Hellström, P. Soriano, Early myotome specification regulates PDGFA expression and axial skeleton development. *Development* **127**, 5059–5070 (2000).